Biochimica et Biophysica Acta, 426 (1976) 101–122

BBA 77205

INTRAMEMBRANE PARTICLE AGGREGATION IN ERYTHROCYTE GHOSTS

II. THE INFLUENCE OF SPECTRIN AGGREGATION*

ARNLJOT ELGSAETER**, DAVID M. SHOTTON*** and DANIEL BRANTON***

Department of Botany, University of California, Berkeley, Calif. 94720 and The Biological Laboratories, Harvard University, 16 Divinity Ave., Cambridge, Mass. 02138 (U.S.A.)

(Received July 7th, 1975)
(Revised manuscript received October 28th, 1975)

SUMMARY

Physicochemical properties of mixtures of spectrin and actin extracted from human erythrocyte ghosts have been correlated with ultrastructural changes observed in freeze-fractured erythrocyte membranes.

(1) Extracted mixtures of spectrin and actin have a very low solubility (less than 30 μg/ml) near their isoelectric point, pH 4.8. These mixtures are also precipitated by low concentrations of Ca^{2+}, Mg^{2+}, polylysine or basic proteins.

(2) All conditions which precipitate extracts of spectrin and actin also induce aggregation of the intramembrane particles in spectrin-depleted erythrocyte ghosts. Precipitation of the residual spectrin molecules into small patches on the cytoplasmic surface of the ghost membrane is thought to be the cause of particle aggregation, implying an association between the spectrin molecules and the intramembrane particles.

(3) When fresh ghosts are exposed to conditions which precipitate extracts of spectrin and actin, only limited particle aggregation occurs. Instead, the contraction of the intact spectrin meshwork induced by the precipitation conditions compresses the lipid bilayer of the membrane, causing it to bleb off particle-free, protein-free vesicles.

(4) The absence of protein in these lipid vesicles implies that all the proteins of the erythrocyte membrane are immobilized by association with either the spectrin meshwork or the intramembrane particles.

---

* Paper I in this series is Elgsaeter and Branton [20].

** Present Address: Institute of Biophysics, University of Trondheim, N-7034 Trondheim-NTH, Norway.

*** To whom reprints requests should be addressed at their current address at the Biological Laboratories, Harvard University.

INTRODUCTION

Spectrin is a major protein component of the mammalian erythrocyte membrane [1–6] located on the membrane's cytoplasmic surface [7]. It appears to be an α-β dimer of two large polypeptide chains with molecular weights of approximately 240000 and 220000, which together comprise about 25 % of the total protein of the membrane [6, 8–10]. These two polypeptides are the two slowest moving bands, bands 1 and 2, seen when the proteins of the erythrocyte membrane are fractionated on sodium dodecyl sulfate-polyacrylamide gels [4, 11]. (The nomenclature of Steck [16] is used throughout this paper to identify the major polypeptides of the erythrocyte membrane.)

Spectrin is thought to play a major role in determining many of the biophysical properties of the erythrocyte, particularly the shape and viscoelastic properties of the cell membrane [12–15]. Most of the spectrin molecules (bands 1 and 2), together with erythrocyte actin (band 5), a smaller protein of molecular weight approximately 43000 which closely resembles muscle actin (Sheetz, M. P., Painter, R. G. and Singer, S. J., personal communication, cited in ref. 16) [17], can be selectively removed from their normal location on the cytoplasmic surface of the membrane by dialysis of erythrocyte ghosts against low ionic strength buffers in the presence of EDTA [1, 2, 4, 6, 10, 18, 19]. During spectrin and actin removal, the ghosts lose their characteristic biconcave shape and become spherical and fragile, eventually vesiculating into smaller membrane fragments.

Our investigations of the human erythrocyte ghost support the suggestion that spectrin plays an important structural role in the membrane. We have shown [20] that substantial amounts of spectrin and actin must be removed from the membrane before the intramembrane particles exposed by freeze-fracture can be induced to aggregate in response to changes of pH or ionic strength. Furthermore, we were struck by the apparent correspondence between the reported values for the isoelectric pH of spectrin (pH 5.3 [1]; approx. pH 4.5 [5]) and the pH range (4.0–5.5) that induced maximal particle aggregation. These investigations of particle aggregation led us to propose that the spectrin, perhaps together with the actin, forms a meshwork on the cytoplasmic surface of the erythrocyte membrane that limits the translational mobility of other membrane macromolecules. On the basis of this spectrin meshwork model, we predicted that simple manipulations, dependent for their effects solely upon the physicochemical properties of spectrin and actin, would induce marked alterations in erythrocyte ghost morphology and ultrastructure. In particular, we predicted that contraction of the spectrin meshwork would lead to expulsion of protein-free lipid vesicles from ghost membranes. We now report experiments which verify this prediction, and describe some of the solubility, electrostatic and aggregation properties of extracted mixtures of spectrin and actin.

METHODS AND MATERIALS

Preparation of erythrocyte ghosts

Ghosts used for electron microscopic investigations were prepared by the procedure of Dodge et al. [21] from small volumes of blood freshly drawn from healthy adult volunteers, as previously described [20].

When large quantities of human erythrocyte ghosts were required for extrac-

tion of spectrin and actin, these were prepared from outdated (21- to 28-day-old) blood-bank blood. The erythrocytes in one bag (450 ml) of blood were washed twice in 1500 ml of phosphate-buffered saline (145 mM NaCl in 20 mosM buffer, pH 7.6), and once in 1500 ml of 310 mosM sodium phosphate buffer (pH 7.6) at 0–4 °C. One bag of blood yielded 90–100 ml of washed erythrocytes, which were lysed in 5 l of 20 mosM sodium phosphate buffer (pH 7.6) while stirring on ice for 15 min. The ghosts were harvested in a Sorvall RC2-B centrifuge using a Szent-Gyorgyi and Blum continuous flow apparatus at 0–4 °C and 17000 rev./min ($35000 \times g$), with a flow rate of 90–110 ml/min. The ghost pellets, but not the red sticky "buttons" of lymphocytes and other cell debris found under them, were resuspended in 5 l of ice-cold 20 mosM sodium phosphate buffer (pH 7.6) and recentrifuged to yield washed ghosts, which were a very pale cream-pink color.

Pretreatment

The term pretreatment is used throughout this paper in the technical sense defined by Elgsaeter and Branton [20] to mean an incubation which depletes the spectrin and actin components of the erythrocyte ghost membrane. Such pretreatment does not by itself cause particle aggregation, but does render the intramembrane particles more susceptible than those of fresh ghosts to subsequent aggregation induced by other treatments (see ref. 20). For the experiments described in this paper, pretreatment consisted of incubating fresh ghosts at 37 °C in 20 mosM sodium phosphate buffer, either at pH 7.6 for 22 h, or at pH 9.0 for 10 h. In both cases 0.5 mM NaN_3 was included to prevent bacterial growth. Pretreatment removed 25–30 % of the total ghost protein, yielding pretreated ghosts devoid of essentially all their actin and roughly 70–80 % of their spectrin [20]. In contrast, the term non-preteated ghosts refers to fresh ghosts containing their full complement of actin and spectrin.

Extraction of erythrocyte spectrin and actin

The washed ghosts from one bag of recently outdated blood have a total of approx. 400 mg protein, as determined by Lowry protein assay [22]. To liberate almost all the spectrin and actin from these ghosts, they were suspended in 55 ml of ice-cold distilled water and dialysed against 5 l of 2 mosM sodium phosphate buffer (pH 9.6) on ice for 24–36 h. To avoid subsequent precipitation of $Ca_3(PO_4)_2$ or $Mg_3(PO_4)_2$, solutions of spectrin and actin intended for divalent cation precipitation experiments were prepared by dialyzing the ghosts against 1 mM Tris · HCl buffer (pH 9.6) instead of the 2 mosM sodium phosphate buffer (pH 9.6). To liberate entrapped molecules from the vesiculated ghosts, the dialysed suspension was sonicated for 30 s at 50 W with a Branson Sonifier (Model 185W). The suspension was then centrifuged at $240000 \times g$ (60000 rev./min in a Beckman 75Ti rotor) for 60 min at 0–4 °C, the pellet discarded, and the supernatant centrifuged at $240000 \times g$ for a further 60 min at 0–4 °C to ensure complete removal of small vesicles. The protein concentration of this second supernatant ranged between 1.5 and 2.1 mg/ml in different preparations and had a faint yellow-orange color. Analysis on sodium dodecyl sulfate gels (see Fig. 1b) of both the phosphate- and the Tris-buffered extracts showed spectrin and actin to be the only major proteins present. Spectrin comprised at least 85 % of the total mass of the extracted protein, and there was only minor (<3 %) contamination by haemoglobin and high molecular weight poly-

peptides. This mixture was used without further fractionation in the precipitation experiments described below.

Titration of mixtures of spectrin and actin

To obtain a solution of spectrin and actin which, by titration, could be used to calculate the charge on an erythrocyte membrane, ghosts were prepared as described above, except that the final wash of the ghosts was in 10 mM NaCl + 2 mosM sodium phosphate buffer (pH 7.6) rather than 20 mosM sodium phosphate buffer (pH 7.6). Spectrin and actin were extracted from these ghosts by dialysis on ice for 40 h against 5 l of 1 mM NaCl adjusted to pH 9.0 with NaOH. Sonication and double centrifugation as described above yielded a solution of spectrin and actin which was then dialysed on ice for a further 68 h against several changes of 1 mM NaCl in glass-distilled water adjusted to pH 9.0 with NaOH, to ensure removal of phosphate ions. Uptake of CO_2 from the air during dialysis was prevented by continuously bubbling N_2 gas through the NaCl solution. The final protein concentration of the dialysed protein mixture was 2.1 mg/ml. 25 ml of this solution were removed and the remainder (17 ml) was adjusted to be 50 mM in NaCl by the addition of 1 M NaCl. Each portion was then separately titrated at 24 °C from pH 9.5 to pH 4.0 with 0.050 M HCl, using a Brinkman pH-stat E415-E512, at a rate of 0.2 pH units/min while stirring on ice. Two 25 ml samples of the final solution against which the protein mixture had been dialysed were similarly titrated as controls. The experimental and blank solutions were analyzed for phosphate [23] and were each found to contain less than 0.03 mM phosphate.

Formation and isolation of particle-free vesicles

Fresh ghosts were induced to bleb and produce particle-free vesicles by incubation in 20 mosM sodium phosphate buffer solutions containing polylysine or protamine sulphate (see figure legends for specific details). Following incubation, extensive vesiculation could be observed by phase contrast light microscopy, spherical or elongated vesicles (diameter 0.5–4 μm) being attached to the external surface of most ghosts. To isolate these vesicles, the vesiculating preparation was forced rapidly through a 27-gauge hypodermic needle, shearing the vesicles from the ghosts. The vesicles and ghosts were then either concentrated by centrifugation at $100\,000 \times g$ (40 000 rev./min in a Beckman 75 Ti rotor) for 30 min at 0–4 °C and separated from each other on a linear sucrose density gradient, or simultaneously concentrated and separated by accelerated flotation using a sucrose step gradient. The linear sucrose density gradient ranged from 1.00 to 1.16 g/cm^3 and was formed by mixing 20 mosM sodium phosphate buffer (pH 7.6) with 20 mosM sodium phosphate buffer (pH 7.6) containing sucrose. After 15 h centrifugation at $80\,000 \times g$ (25 000 rev./min in a Beckman SW27 rotor) at 0–4 °C, the vesicles formed two low-density bands at positions corresponding to densities of 1.03 and 1.05 g/cm^3, while the ghost membranes formed a high-density band at the bottom of the tube. The step gradient was formed by adding sufficient solid sucrose directly to the sheared vesicles and ghosts to bring the mixture to a density of 1.09 g/cm^3. This mixture was then overlaid with 20 mosM sodium phosphate buffer (pH 7.6) and centrifuged for 90 min at $80\,000 \times g$ at 0–4 °C. Under these conditions, the ghosts pelleted to the bottom of the tube while the vesicles floated to the interface between the sucrose solution and the overlay.

Immunochemical labelling

Rabbit anti-phenyllactoside antibody, directed against the hapten *p*-azophenyl-β-D-lactoside, was isolated by affinity chromatography [24] from the serum of rabbits inoculated with keyhole limpet haemocyanin which had been heavily labelled by diazotization with *p*-diazoniumphenyl-β-D-lactoside [25]. It was made fluorescent by reaction with fluorescein isothiocyanate [26], and then conjugated to ferritin with glutaraldehyde [27].

Fresh intact erythrocytes were diazotized with *p*-diazoniumphenyl-β-D-lactoside by a modification [28] of the method employed to couple aminophenyl glycosides to polyacrylamide beads [29]. This procedure leads to the non-specific hapten modification of tyrosine and histidine residues of proteins exposed on the outer surface of the erythrocyte membrane. Full descriptions of these preparations will be presented in a subsequent paper (Shotton, D. M., Thompson, K., Wofsy, L. and Branton, D., manuscript in preparation). Ghosts were prepared from these phenyllactoside-modified erythrocytes as described previously [20, 21] and were labelled with the conjugated anti-phenyllactoside antibody, as described in the legend to Fig. 10, after protamine induction of lipid vesicle blebbing.

Freeze-etch electron microscopy

Freeze-fracturing or freeze-etching was done by standard techniques [30] in a Balzers apparatus (Balzers High Vacuum Corp., Santa Ana, Calif., U.S.A.), except that replicas were cast using Pt-C and C anodes heated by electron bombardment from tungsten cathodes [31]. Replicas were cleaned in household bleach, mounted on bare 400-mesh grids and examined in a Siemens 1A or a Phillips 301 electron microscope.

Sodium dodecyl sulfate-polyacrylamide gel electrophoresis

The procedures used were essentially those of Fairbanks et al. [4], with the minor modifications described by Elgsaeter and Branton [20].

RESULTS

Since spectrin and actin molecules exist together on the cytoplasmic surface of the membrane [16] and together may form a meshwork controlling the distribution and mobility of the membrane-intercalated proteins [20, 17] and of the anionic sites on the outer surface of the membrane [32], we thought it worth while to study the solubility properties of extracted mixtures of these two proteins and to relate them to our studies of intramembrane particle aggregation. Although no functional relationship between spectrin and actin has yet been firmly established, we decided to study them together, in approximately the same stoichiometry in which they are found on the membrane. This study, therefore, does not distinguish between the separate contributions of spectrin and actin to the solubility properties of the mixture.

Solubility properties

We found the isoelectric point for the extracted mixture of spectrin and actin in 20 mosM sodium phosphate buffer to be pH 4.8, at which pH the protein solubility is only 25–30 μg/ml (Fig. 1). In phosphate-buffered saline, precipitation occurs over

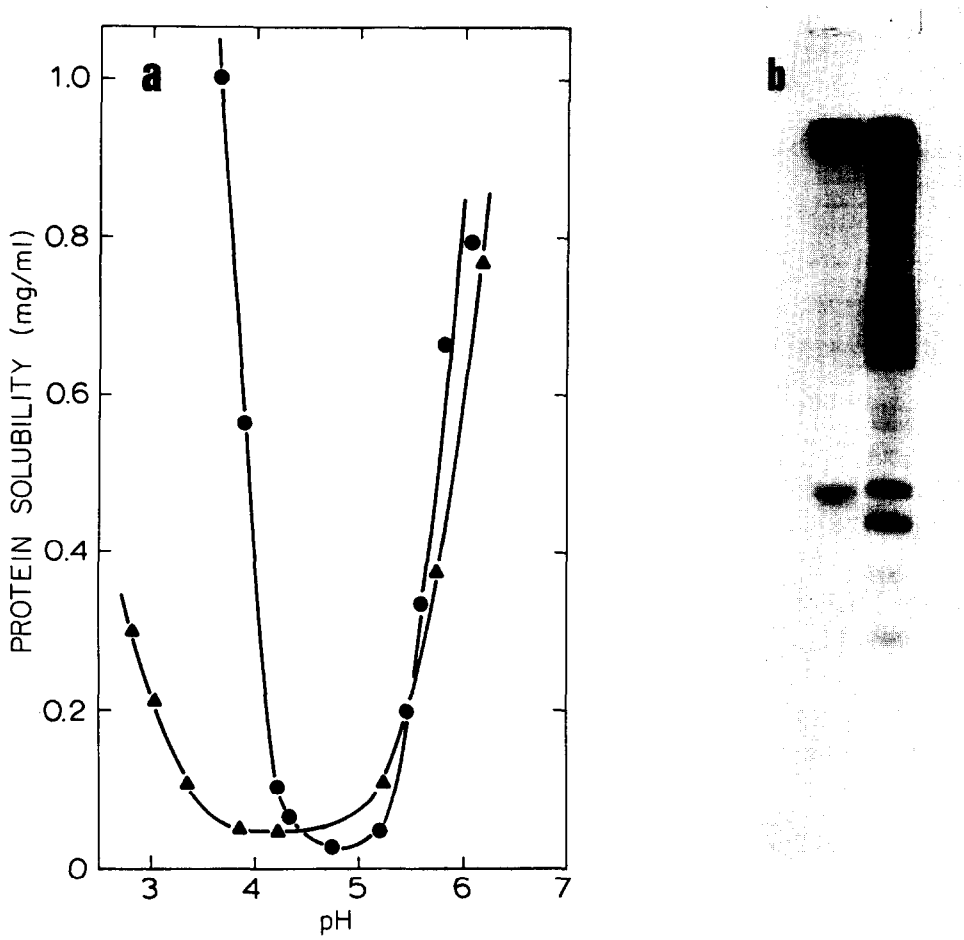

Fig. 1. (a) The isoelectric precipitation curves of an extracted mixture of spectrin and actin in 20 mosM sodium phosphate buffer (●) and in phosphate-buffered saline (▲) at 0 °C. Two samples of the solution of spectrin and actin were dialysed overnight against ice-cold 20 mosM sodium phosphate buffer (pH 7.6). 1 M NaCl was then added to make one of these solutions 145 mM in NaCl, and both solutions were adjusted to pH 8.5 with 0.1 M NaOH. Each solution (approx. 50 ml) was then titrated slowly with 0.1 M HCl from pH 8.0 to pH 2.8, while gently stirring on ice. Samples were taken at different pH values, allowed to stand for at least 5 h on ice (duplicate experiments using lesser time periods gave identical results), and then centrifuged at 100 000 × g for 30 min at 0–4 °C. The residual protein concentration in the supernatant was determined by its absorbance at 280 nm, using an extinction coefficient, $E_{280\,nm}^{1\,\%\cdot 1\,cm}$, of 10.0, which was determined for the original protein mixture using the Lowry assay. Similar curves were obtained at room temperature. (b) Coomassie brilliant blue-stained sodium dodecyl sulfate-polyacrylamide gels of fresh ghosts (right gel, 50 μg protein) and of the extracted mixture of spectrin and actin used in these solubility studies (left gel, 10–15 μg protein). The gels were run together and stained identically.

a broader pH range, from about pH 3.8 to pH 5.3. In both 20 mosM sodium phosphate buffer and phosphate-buffered saline the white flocculent isoelectric precipitate could be easily solubilized by lowering the pH below 3.5 or raising it above 6.0, the isoelectric precipitation curves themselves showing a hysteresis of 0.2–0.3 pH units

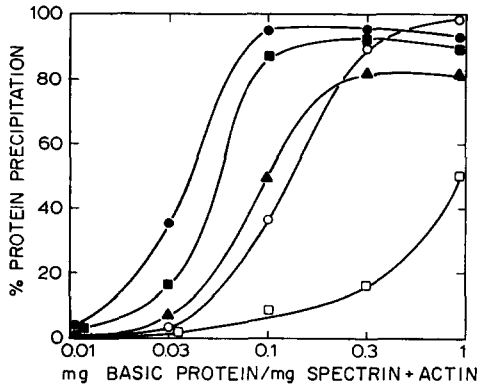

Fig. 2. Precipitation of spectrin and actin by polylysine, M_r 41 600 (●); polylysine, M_r 4 000 (■); lysine-rich histone (▲); protamine sulphate (Sigma) (○); and trypsin (twice crystallized, Sigma) (□). 100 μl of different concentrations of these polycations or basic proteins in 20 mosM sodium phosphate buffer (pH 7.6) were added to separate but identical 2 ml samples of a 0.3 mg/ml solution of spectrin and actin in the buffer. After standing for 30 min on ice the mixtures were centrifuged at 0–4 °C for 30 min at 100 000 × g. In the case of trypsin, however, the active enzyme was dissolved in ice-cold 1 mM HCl (the HCl causing a change of less than 0.2 pH units when added to the spectrin/actin mixture), and the samples to which it was added were centrifuged at 0–4 °C immediately after addition, to avoid proteolysis. The absorbances at 280 nm of the supernatants were measured, and the percent of total protein which had precipitated was calculated from the known absorbances of the original solution of spectrin and actin and of the various polycation or basic protein solutions added to it.

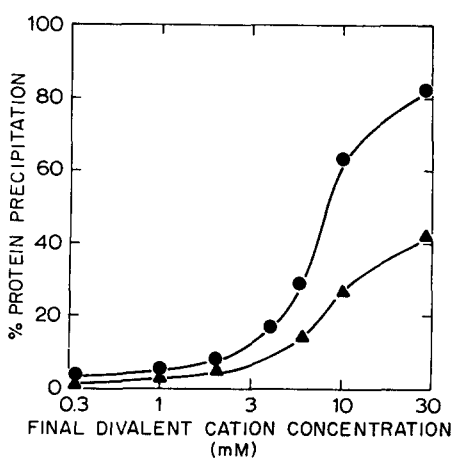

Fig. 3. Precipitation of spectrin and actin by $CaCl_2$ (●) and $MgCl_2$ (▲). 100 μl of different concentrations of $CaCl_2$ or $MgCl_2$ in 8 mM Tris (pH 7.6) were added to separate but identical 2 ml samples of a 0.5 mg/ml Tris-extracted solution of spectrin and actin in 8 mM Tris (pH 7.6). After standing for 30 min on ice, the mixtures were centrifuged at 0–4 °C for 30 min at 100 000 × g, and the percent protein precipitated was determined by measuring the absorbances of the supernatants at 280 nm. The Tris-extracted proteins used for these experiments gave a sodium dodecyl sulfate-polyacrylamide gel pattern indistinguishable from that shown in Fig. 1b.

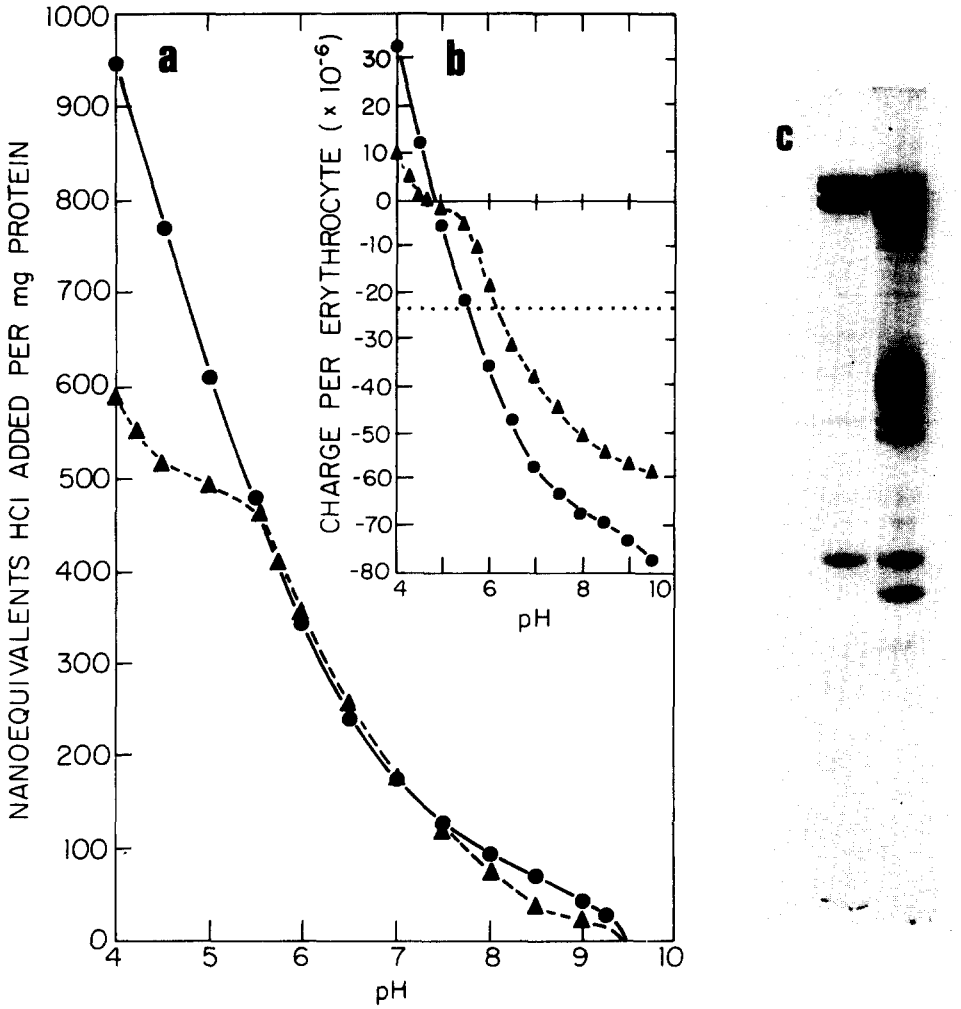

Fig. 4. Titration of spectrin and actin. (a) Samples of a buffer-free preparation of spectrin and actin, in 1 mM NaCl (—) and in 50 mM NaCl (- - -), were titrated at 24 °C from pH 9.5 to pH 4.0 with 0.050 M HCl. The titration curves were corrected for the amount of HCl needed to titrate blank samples of the final solution against which the protein mixture had been dialyzed, the corrections being between 8 and 12 % at different points across the pH range. (b) The contribution which spectrin and actin make to the electrostatic charge, expressed in electrostatic units, on an erythrocyte membrane in 1 mM NaCl (—) or in 50 mM NaCl (- - -) was calculated from the corrected titration curves, assuming that the net charge on the molecules in the spectrin/actin mixture is zero at the isoelectric point of the mixture (pH 4.8), that there are approx. $1.96 \cdot 10^{-10}$ mg of spectrin and actin per erythrocyte, and that the titration behavior of these proteins on the membrane resembles that in solution. For comparison, the charge that would be contributed by the total number of sialic acid residues (approx. $2.4 \cdot 10^7$ per human erythrocyte, according to Eylar et al. [57] is also shown (· · ·). This is constant over the pH range 4–10, since the pK_a of sialic acid is 2.6 [58]. (c) Coomassie brilliant blue-stained sodium dodecyl sulfate-polyacrylamide gels of fresh ghosts (right gel, 50 μg protein) and of the buffer-free protein mixture used for the titration studies (left gel, 10–15 μg protein). The gels were run together and stained identically.

upon reversing the direction of titration. The precipitation time allowed before centrifugation at each pH value was not critical within 0.5–5.0 h. The mixture of spectrin and actin could also be precipitated by polycations such as polylysine, or basic proteins such as protamine or histone (Fig. 2). Even trypsin, a less basic protein with an isoelectric point of pH 10.1 [33], effectively precipitated the extracted proteins under conditions where proteolysis by trypsin was negligible. Millimolar concentrations of Ca^{2+} or Mg^{2+} also caused these proteins to precipitate (Fig. 3), Ca^{2+} being about twice as effective as Mg^{2+}. Clarke [5, 6] reported Ca^{2+} to be even more effective in precipitating purified bovine spectin.

Electrostatic charge

All our investigations of particle aggregation [20] and of the solubility of mixtures of spectrin and actin (vide supra) suggested that electrostatic interactions between these proteins play a major role in controlling the physical properties of the erythrocyte membrane. We therefore titrated these extracted proteins (Fig. 4a) and calculated the contribution that spectrin and actin would make to the total electrostatic charge on an erythrocyte membrane as a function of pH (Fig. 4b). The calculation assumes that the total protein content of a haemoglobin-free ghost is

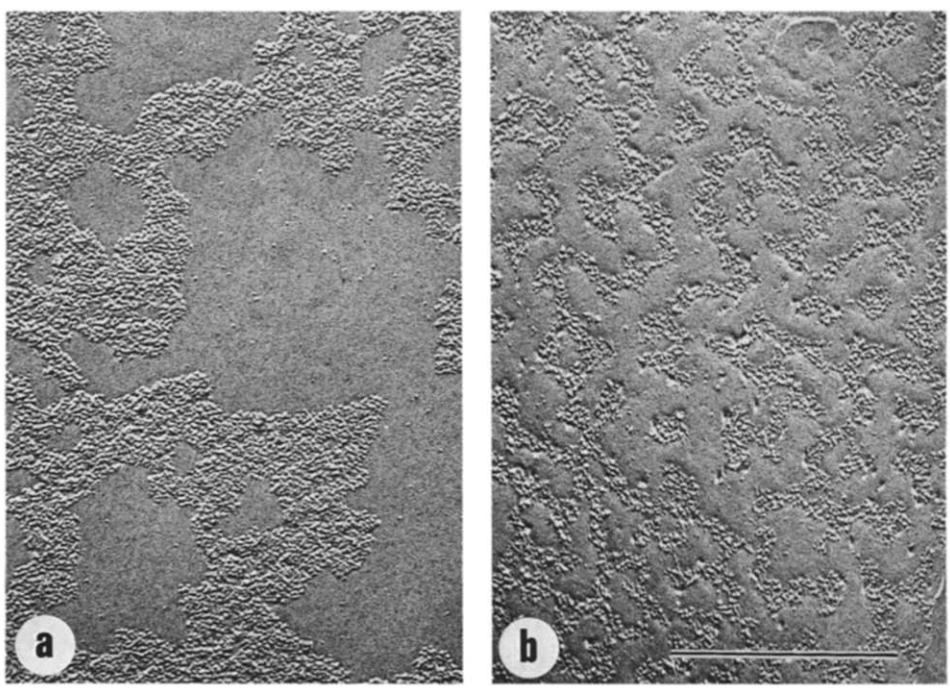

Fig. 5. Freeze-etch electron micrographs (×60 000) showing particle aggregation induced by basic protein in (a) pretreated and (b) fresh ghosts. 0.1 ml of the pretreated or fresh ghosts was incubated for 30 min at 0 °C in 1 ml of 20 mosM sodium phosphate buffer (pH 7.6) containing protamine sulphate (0.3 mg/mg residual membrane protein for pretreated ghosts, or 1.0 mg/mg membrane protein for fresh ghosts). The ghosts were then frozen, freeze-fractured and etched for 1 min at −100 °C prior to replication. Extensive lipid vesicle blebbing (see Fig. 6) was induced in the fresh ghosts (b), but not in the pretreated ghosts (a). Bar = 5 000 Å.

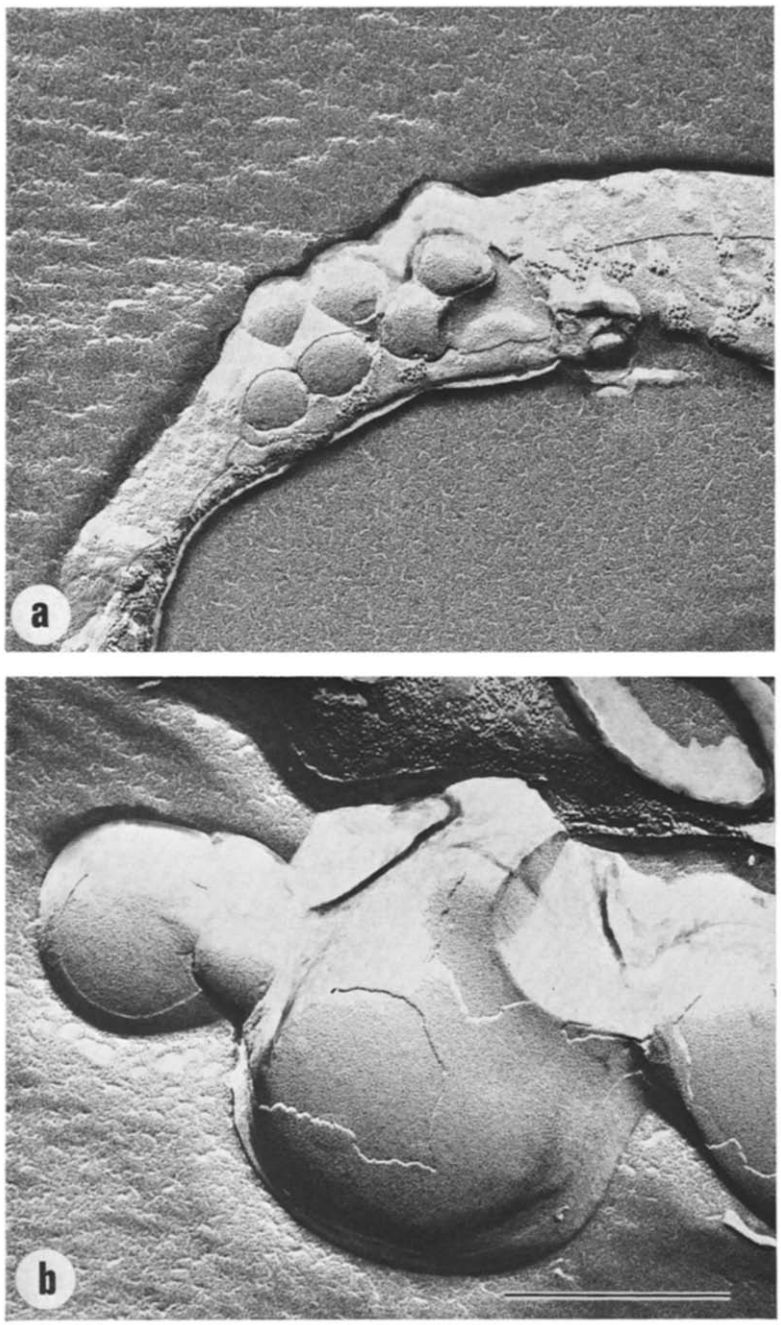

Fig. 6. Freeze-etch electron micrographs (× 60 000) illustrating particle-free lipid vesicle formation in (a) non-pretreated ghosts and (b) non-pretreated phenyl lactoside-modified ghosts. Here limited particle aggregation and extensive vesicle blebbing were induced by incubating 0.1 ml of packed ghosts for 30 min at 0 °C in 2 ml of 20 mosM sodium phosphate buffer (pH 7.6) containing 0.1 mg of protamine sulphate. The ghosts were then frozen, freeze-fractured and etched for 1 min at −100 °C prior to replication. Figs. 6a and 6b have been chosen to illustrate early and late stages in lipid vesicle blebbing, no differences in the degree of particle aggregation or vesicle formation being observed between normal and phenyl lactoside-modified ghosts. Bar = 5 000 Å.

$5.7 \cdot 10^{-10}$ mg, and that the percentages of bands 1, 2 and 5 are 15.1 %, 14.7 % and 4.5 %, respectively [16]. Spectrin and actin therefore comprise approx. 35 % of the total membrane protein, or $1.96 \cdot 10^{-10}$ mg per ghost. Comparison with the charge contributed by sialic acid (Fig. 4b) shows that at physiological pH values the spectrin and actin contribute as much to the charge on the inside surface of the erythrocyte membrane as does sialic acid to the outside surface.

Formation and isolation of particle-free vesicles

When pretreated ghosts were incubated with any of the basic proteins we knew to be effective in precipitating mixtures of spectrin and actin (vide supra), extensive aggregation of the intramembrane particles occurred (Fig. 5a). In contrast, when fresh, non-pretreated ghosts were exposed to basic proteins, only moderate

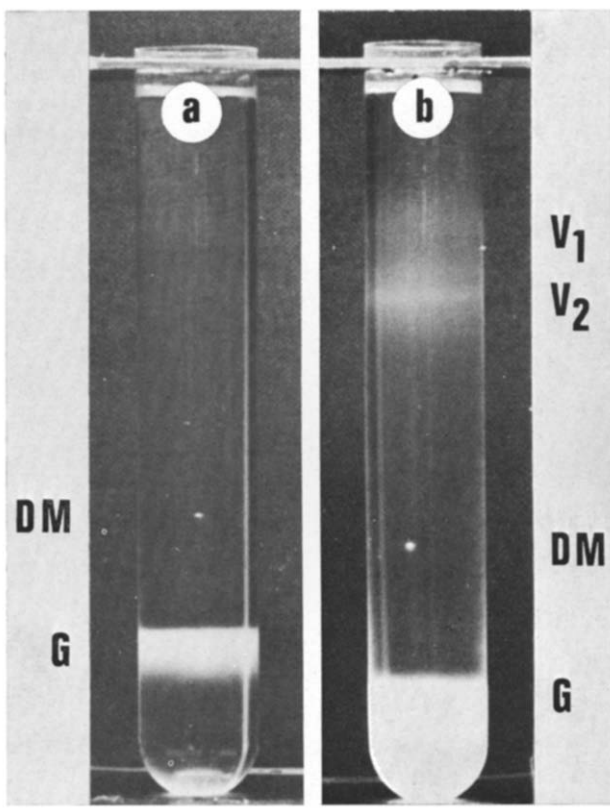

Fig. 7. Sucrose density gradients of fresh ghosts (a) and of polylysine-treated, vesiculated ghosts (b). Two 1 ml samples of fresh ghosts were separately incubated for 45 min at 37 °C in 11 ml of 20 mosM sodium phosphate buffer (pH 7.6) with and without 2.5 g polylysine (M_r 4 000). After shearing by passage through a 27-gauge hypodermic needle, and centrifugation, the pellets were each resuspended in 1 ml of ice-cold 20 mosM sodium phosphate buffer (pH 7.6) layered on top of linear 1.00–1.16 g/cm^3 sucrose density gradients and centrifuged at 0–4 °C for 15 h at 80 000 $\times g$. The polylysine-induced lipid vesicles formed two low density bands at positions corresponding to densities of 1.03 and 1.05 g/cm^3 (V_1 and V_2, right). No such vesicles were formed from the sheared ghosts which had not been treated with polylysine (left) although both tubes contained a high density band of ghosts (G). A density marker bead ((DM, ρ = 1.10 g/cm^3) was included in each tube.

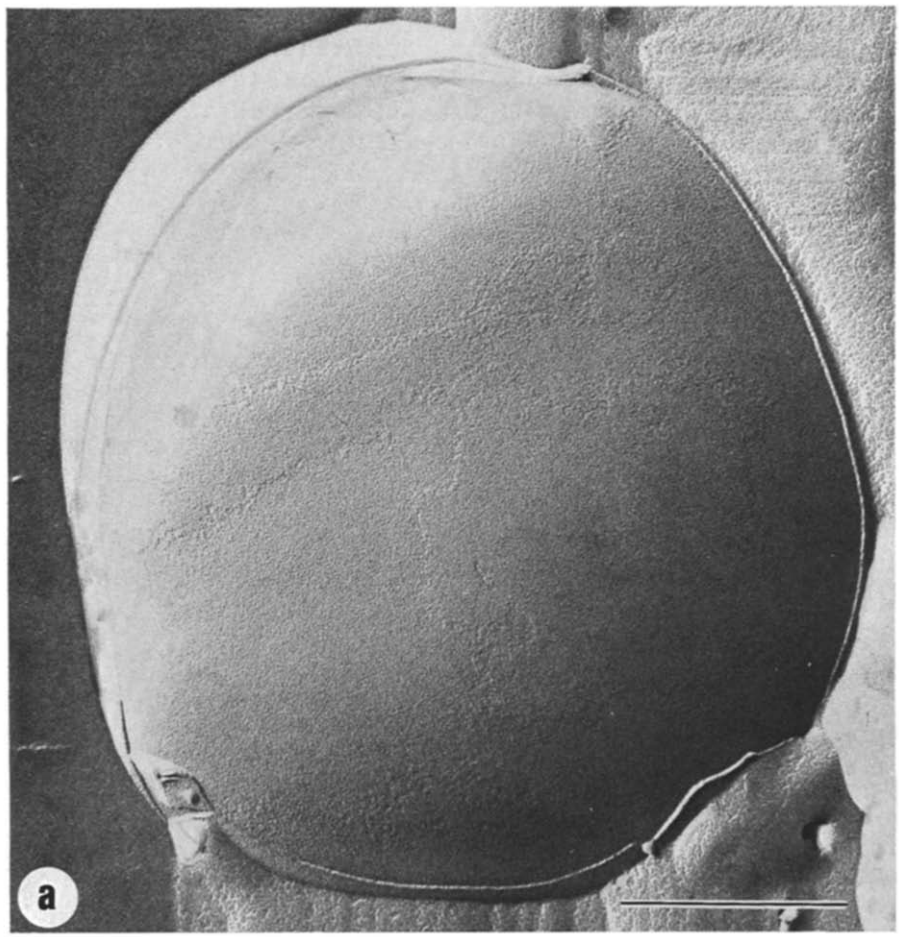

particle aggregation occurred, even if greater amounts of the basic protein were employed (Fig. 5b). Instead, blebbing occurred and small vesicles were pinched off from the ghost surface (Fig. 6). Although nearly every ghost produced vesicles, less than 10 % of the initial ghost surface area appeared to be pinched off. The blebs and vesicles were devoid of intramembrane particles and were similar in appearance to pure phospholipid vesicles [34], occasionally showing multilamellar fracture faces. Similar large vesicles were observed when fresh ghosts were exposed to concentrations of Ca^{2+} greater than 5 mM, and small particle-free blebs with diameters up to 1000 Å appeared when fresh ghosts were treated with phosphate-buffered saline whose pH had been adjusted to 5.0.

Since the phenomena of ghost pretreatment, particle aggregation, spectrin precipitation and vesicle blebbing seemed to be so closely related, we isolated some of these particle-free vesicles for further study on a sucrose density gradient (Fig. 7). The particle-free vesicles formed two low density bands on the gradient. The upper of these two low density bands (Fig. 8a) contained larger vesicles than did the lower

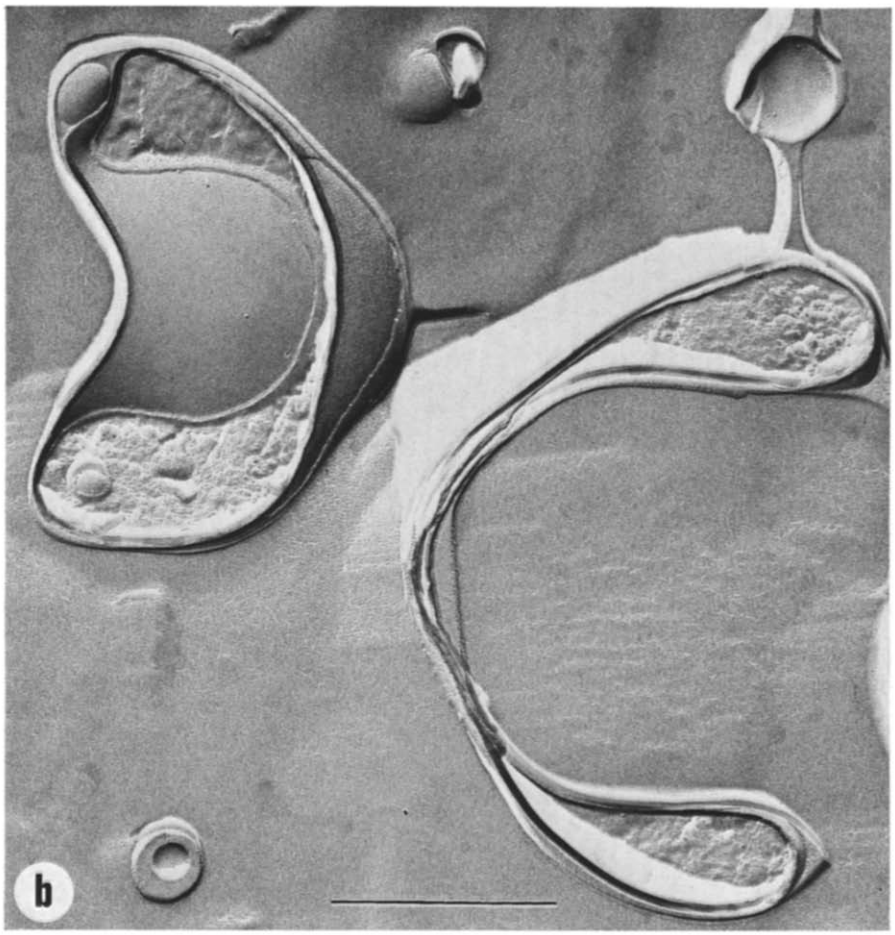

Fig. 8. Freeze-etch electron micrographs (× 60 000) of the particle-free lipid vesicles. The two low-density bands from the density gradient shown in Fig. 7 were separately resuspended in 13.5 ml of 20 mosM sodium phosphate buffer (pH 7.6) and centrifuged at 100 000 × *g* for 30 min at 0–4 °C. Samples of the pellets were frozen, freeze-fractured and etched for 1 min at −100 °C prior to replication. (a) Low density band V_1; (b) low density band V_2. Bar = 5000 Å.

band (Fig. 8b), but no other significant differences were observed.

The protein: lipid weight ratio in the particle-free vesicles was estimated to be less than 0.05 on the basis of the vesicle density. When subjected to sodium dodecyl sulfate-polyacrylamide gel electrophoresis at high loadings and stained with Coomassie brilliant blue (Fig. 9a), only traces of spectrin and a few other very minor bands were apparent. When an identical gel was stained for carbohydrate (Fig. 9b) with periodic acid-Schiff's reagent, no trace of glycophorin, the major erythrocyte sialoglycoprotein [35], was seen, despite the heavy overloading which gave rise to the dense band, probably due to glycolipid, visible in the low molecular weight region of the gel.

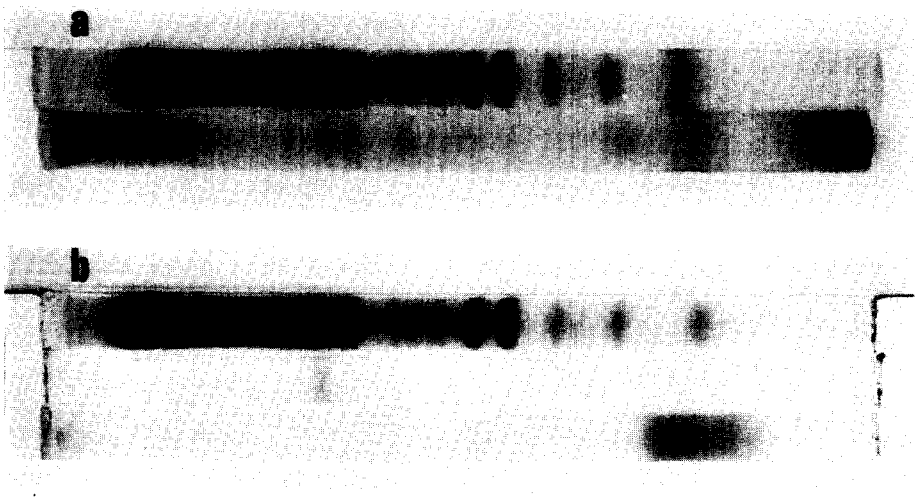

Fig. 9. Sodium dodecyl sulfate-polyacrylamide gels of polylysine-induced lipid vesicles. (a) Coomassie brilliant blue staining: top gel, 10 μl of packed fresh ghosts; bottom gel, 10 μl of packed polylysine-induced lipid vesicles. (b) Top gel, 10 μl of packed fresh ghosts, stained with Coomassie brilliant blue; middle and bottom gels, periodic acid-Schiff staining: middle gel, 10 μl of packed fresh ghosts; bottom gel, 10 μl of packed polylysine-induced lipid vesicles. To prepare the vesicles, 7.5 ml of fresh ghosts were incubated for 45 min at 37 °C in 75 ml of 20 mosM sodium phosphate buffer (pH 7.6) containing 18 mg polylysine (M_r 4 000). After shearing and addition of solid sucrose to a density of 1.09 g/cm^3, giving a final volume of 117 ml, three 39 ml portions were placed in three 40 ml centrifuge tubes, separately overlaid with 1 ml of 20 mosM sodium phosphate buffer (pH 7.6) and centrifuged at 0–4 °C for 90 min at 80 000 × g. The low-density lipid vesicles banded at the sucrose-buffer interface, while the protein-rich ghost membranes formed a pellet at the bottom of each tube. The interfacial bands from the three tubes were combined, washed free of sucrose in 20 mosM sodium phosphate buffer (pH 7.6) and concentrated to yield two 10 μl samples of vesicles, which were then dissolved in sodium dodecyl sulfate and electrophoresed. The gels in each group (a and b) were run and stained in parallel.

Immunochemical labelling

Direct visualization of the in-plane distribution of surface proteins was achieved by applying ferritin-conjugated, fluorescein-labelled anti-phenyl lactoside antibody to ghosts prepared from erythrocytes whose outer surface proteins had been modified by phenyl lactoside hapten. When the intramembrane particles of the

Fig. 10. Immunochemical labelling of surface proteins on phenyl lactoside modified ghosts. Freeze-etch electron micrographs (× 60 000) of ferritin-anti-phenyl lactoside-labelled preparations of non-pretreated phenyl lactoside-modified ghosts in which limited particle aggregation and extensive lipid vesicle blebbing was induced by protamine. (a), (b) and (c) show progressive stages of vesicle blebbing. Fracture faces (F) are devoid of particles and etched surfaces (S) are devoid of ferritin-conjugated antibody molecules (A) beyond the necks of the blebbing vesicles. (d) A rare vesicle with small clumps of ferritin-conjugated antibodies molecules. To prepare these specimens, vesiculation was first induced by protamine treatment, as described in the legend for Fig. 6. The vesiculating phenyl lactoside-modified ghosts were then concentrated by centrifugation at 10 000 rev./min (12 000 × g) for 10 min, and labelled by incubating 40 μl of the ghost pellet on ice for 2 h with 200 μl of ferritin-conjugated fluorescein-labelled anti-phenyl lactoside in phosphate-buffered saline. After washing twice to remove excess unbound antibody by diluting to 2 ml with phosphate-

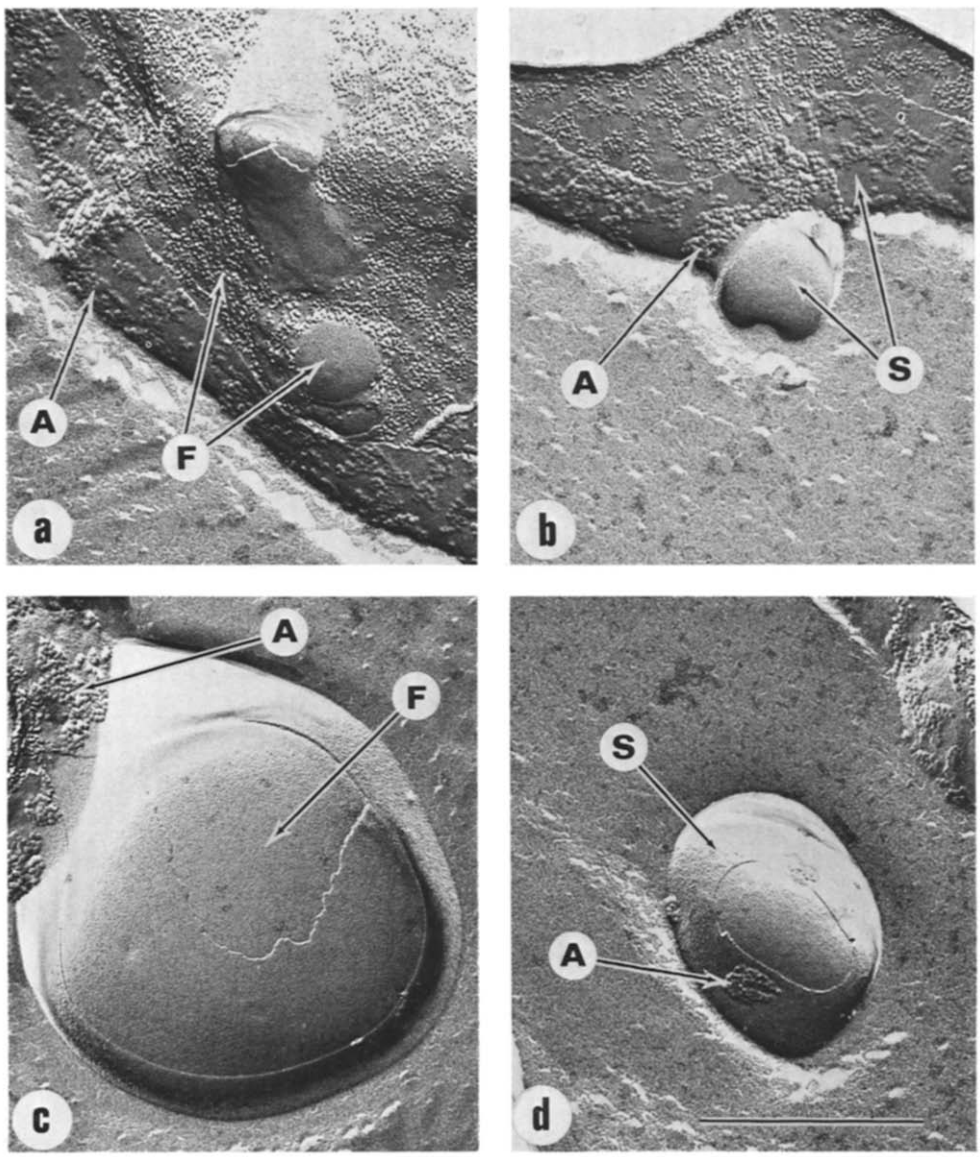

buffered saline and pelleting at 10 000 rev./min for 10 min at 0–4 °C, the labelled phenyl lactoside-modified ghosts appeared intensely fluorescent against a dark background when examined in a fluorescence microscope, while control samples of normal, non-phenyl lactoside-modified ghosts showed no fluorescence. Specimens were frozen in phosphate-buffered saline, freeze-fractured and etched for 90 s at −100 °C before replication. In spite of the relatively high salt content of phosphate-buffered saline, the ghosts were not completely entrapped in the NaCl eutectic-like phase, as they would have been in other solutes (compare with Fig. 1 in ref. 59). The eutectic-like NaCl phase obscured the etched ghost surfaces only in clearly distinguishable, localized areas, and much of the ghost surface area was exposed normally by etching, as if the ghosts were in water or a low ionic strength buffer. (See Fig. 6 for non-phenyl lactoside and phenyl lactoside-modified ghost controls which have been similarly induced to vesiculate, but which have been freeze-fractured without prior immunochemical labelling by ferritin-anti-phenyl lactoside). Bar = 5000 Å.

ghosts were induced to aggregate, a very strong positive correlation was found between the distribution of the intramembrane particles on the fracture face and the ferritin molecules on the adjacent external etched surface (Shotton, D. M., Thompson, K., Wofsy, L. and Branton, D., manuscript in preparation). This suggests that all the labelled outer proteins are associated with and aggregate with the intramembrane particles.

When protamine-treated, phenyl lactoside-modified ghosts in the process of blebbing particle-free lipid vesicles were similarly labelled, the ferritin-conjugated anti-phenyl lactoside was seen in small patches on the ghost membrane above the partially aggregated intramembrane particles (Fig. 10). In contrast, the lipid blebs usually appeared to be totally devoid of both ferritin molecules and intramembrane particles (Figs. 10a, 10b and 10c). A very small proportion of vesicles (approx. 0.1 %) showed small clumps of ferritin molecules on their surfaces (Fig. 10d). These few protein-bearing vesicles presumably contribute the traces of protein observed by sodium dodecyl sulfate-polyacrylamide gel electrophoresis of the purified vesicles described above (Fig. 9).

DISCUSSION

Spectrin precipitation and particle aggregation

Our previous report [20] described two steps required to aggregate the intramembrane particles of erythrocyte ghosts: a pretreatment which removed a substantial portion of the spectrin and actin from the ghost but did not alter the normal dispersed distribution of the particles, and a subsequent exposure of these pretreated ghosts to conditions which induced aggregation of the intramembrane particles. Ghosts which had not been pretreated showed little or no particle aggregation when exposed to the same aggregating conditions. This and other observations led us to propose that pretreatment loosens up a spectrin meshwork which normally constrains the intramembrane particles in an immobilized dispersed state.

In this paper we have described complementary studies on the spectrin and actin mixture removed from erythrocyte ghosts by our pretreatments. We found that all conditions which are effective in causing particle aggregation in pretreated ghosts are also effective, to a similar degree, in precipitating extracted mixtures of these two proteins. For instance, the extracts of spectrin and actin show strong reversible isoelectric precipitation in the pH range 3.8–5.3 (Fig. 1), the same pH range where strong, reversible particle aggregation was found in pretreated ghosts [20]. The solubility of the extracted protein mixture at its isoelectric point, pH 4.8, is only 25–30 μg/ml. If one assumes that the residual spectrin of a pretreated ghost, from which about 80 % of the initially-bound spectrin and almost all the actin have been removed, is located within 1000 Å of the membrane's lipid bilayer, the average local spectrin concentration would be at least 2 mg/ml. (There are approx. 220000 molecules of spectrin per ghost [16]. If 44000 spectrin molecules, molecular weight 460000 [6] remain after pretreatment, and they are confined to a layer 1000 Å thick on the 145 μm^2 inner surface of a ghost membrane, the local spectrin concentration in this layer would be 2.32 mg/ml.) Thus even in pretreated ghosts the local spectrin concentration on the membrane surface is almost two orders of magnitude higher than the solubility limit of an extracted mixture of spectrin and actin at pH 4.8.

Consequently, exposure of pretreated ghosts to low pH would be expected to cause local isoelectric precipitation of the residual spectrin on the cytoplasmic surface of the membrane. If the spectrin is bound to the intramembrane particles, this precipitation would in turn affect the lateral distribution of these particles, causing them to aggregate. Since spectrin can also be precipitated by basic proteins (Fig. 2) and divalent cations (Fig. 3), the addition of these molecules to pretreated ghosts would be expected to cause similar effects. We therefore suggest that under these conditions it is a microprecipitation of the residual spectrin molecules on the cytoplasmic surface of the membranes of pretreated ghosts which is causing the aggregation of the underlying intramembrane particles.

While such an explanation fits our observations well, so little is known of the solubility properties of the components of the intramembrane particles that the possibility of direct effects of pH, divalent cations or basic proteins on the particles themselves cannot be ruled out. It is known that phase separation of lipids can induce particle aggregation [36–38], and since Ca^{2+} or Mg^{2+} is able to induce phase separations in mixed lipid systems [39, 40], such phase separation may also play a role in the particle aggregation observed when ghosts are incubated in divalent and polyvalent cations.

It is important to note that while we induced particle aggregation in pretreated ghosts by procedures which we believe affect spectrin on the cytoplasmic surface of the membrane, there is no reason to suppose that other treatments, for example exposure to polyvalent antibodies directed against antigenic determinants on the outer surface of the pretreated membrane, would not be similarly effective in inducing aggregation. Transmembrane effects have been implicated by studies showing both that anti-spectrin-induced aggregation of spectrin on the inside surface of the ghost membrane can lead to aggregation of negatively charged sites on the outside surface of the ghosts [32], and that induced aggregation of determinants on the outside of the ghost can lead to enhanced cross linking of spectrin on the inside [41]. The exact role of the intramembrane particles in these transmembrane phenomena remains to be explored.

Our data lead us to expect an association between the negatively charged spectrin molecules and the cytoplasmic portions of the intramembrane particles. Many of our observations are consistent with the notion that at low ionic strength (20 mosM or less) electrostatic repulsion between negative charges, both on spectrin and on glycophorin, play a role in preventing particle aggregation in pretreated ghosts. Such repulsion could explain the reversibility of pH-induced particle aggregation when pretreated ghosts in 20 mosM sodium phosphate buffer are returned from pH 5.5 to pH 7.6 [20]. At pH 7.6 the isoelectrically precipitated spectrin molecules will disaggregate and allow electrostatic repulsion and thermal translational effects to disperse the aggregated particles. Similarly, if electrostatic repulsion were important in keeping the intramembrane particles dispersed, it would explain our observations [20] that removal of sialic acid by neuraminidase gives rise to a significant increase in particle aggregation of pretreated ghosts when they are kept in 20 mosM sodium phosphate buffer at all pH values between 4 and 9. It also explains why a significant increase in particle aggregation of pretreated ghosts is observed when they are placed in phosphate-buffered saline at pH values between 4 and 9. The neuraminidase treatment would reduce charge repulsion by removing charged

groups, while the increased salt concentration in phosphate-buffered saline would reduce the efficiency of electrostatic repulsion by Debye shielding.

The spectrin meshwork and the formation of protein-free lipid vesicles

If a spectrin meshwork model correctly describes aspects of the erythrocyte membrane, one would predict that leaky fresh ghosts would distort when exposed to conditions that precipitate extracted mixtures of spectrin and actin. During strong precipitation conditions the spectrin meshwork dimensions would tend to be reduced, and tangential pressure, transmitted via the intramembrane particles and other interactions to the membrane lipid bilayer, would become higher. Since the minimum surface area of the bilayer is determined by the number of lipid molecules it contains, lipid molecules would be forced away from intimate association with the spectrin meshwork once a critical collapse pressure is exceeded. Since phospholipid molecules are capable of rapid lateral motion within the erythrocyte bilayer [42], bulk lateral flow leading to the formation of particle-free phospholipid blebs and vesicles (Fig. 11) would be expected. This would lead to a small reduction of the surface area of the lipid bilayer remaining in association with the spectrin meshwork and thus relieve the compressive strain present in the original bilayer. The formation of such lipid vesicles is exactly what we observed under these conditions (Fig. 6). That the intact spectrin meshwork is essential for the formation of particle-free lipid vesicles is demonstrated by the observation that if 80 % of the spectrin meshwork is first removed by pre-treatment, particle-free lipid vesicles do not form upon addition of basic proteins. Instead, massive particle aggregation occurs (Fig. 5a).

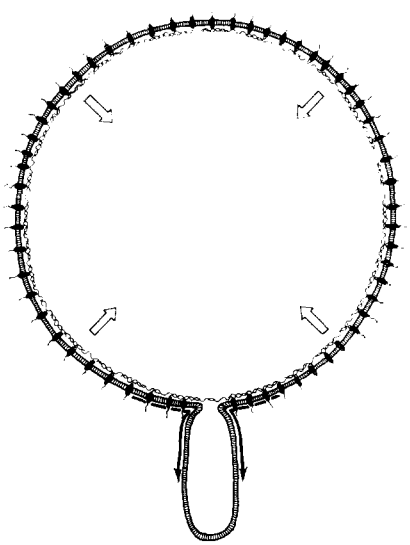

Fig. 11. Illustration of the behavior predicted by the spectrin meshwork model when a leaky fresh ghost is exposed to conditions which cause strong precipitation of extracted mixtures of spectrin and actin. The spectrin meshwork (wavy lines) will contract (open arrows), and since it is closely associated with the phospholipid bilayer (shaded) and the intramembrane particles (black ovals), the compressive force transmitted to the bilayer will cause bulk lateral flow of phospholipid molecules (black arrows) past the immobilized intramembrane particles to form protein-free lipid vesicle blebs (compare with Figs. 6 and 10).

Since the formation of particle-free lipid vesicles involves in-plane bulk flow of lipid into the bleb, any protein floating freely in the lipid bilayer should be carried with this flow of lipid molecules into the forming vesicles. However, analysis of the vesicles by sodium dodecyl sulfate-polyacrylamide gel electrophoresis (Fig. 9) and visualization of surface proteins by immunochemical hapten labelling (Fig. 10) indicate that these vesicles are essentially protein-free. Although we do not know whether the addition of calcium or basic proteins causes abnormal association between the different proteins in the membrane, the simplest interpretation of our data is that all the major proteins of the erythrocyte membrane are normally associated with the intramembrane particles or the spectrin meshwork, the intact meshwork preventing the particles themselves from being swept into the forming vesicles. In contrast, extensive disruption of the spectrin meshwork by prolonged pretreatment of ghosts results in the formation of a different type of vesicle which has the same protein composition as the ghost from which it is derived.

In agreement with our studies, crosslinking studies [43] showing extensive crosslinking of most erythrocyte membrane proteins with spectrin are consistent with a model of transmembrane and cytoplasmic surface proteins anchored to a spectrin meshwork. Furthermore, fluorescence microscopy has shown that the surface proteins of fresh erythrocyte ghosts are not free to diffuse [44]. These results from the erythrocyte membrane thus stand in contrast to the free mobility of membrane proteins implied in the original formulation of the fluid-mosaic model proposed by Singer and Nicolson [45], and found valid for the behavior of certain proteins in other types of cells [46–49].

The spectrin meshwork also has implications concerning a related phenomenon, namely the resealing of leaky ghosts. The resealing effect of Ca^{2+} and Mg^{2+} upon leaky ghosts has been known for a long time, but the mechanism responsible for the effect has so far been unexplained [50, 51]. According to our model, when divalent cations or basic proteins are added to leaky fresh ghosts, the first result of the increased tangential pressure in the membrane due to contraction of spectrin meshwork would be the closing of holes in the lipid bilayer. Shin and Carraway [52] found that trypsin had a resealing effect which is now explicable in light of the fact that trypsin is a basic protein that also causes precipitation of extracted spectrin and actin. The reduction in the volume of ghosts as a result of adding 2 mM Ca^{2+} [53] may be another closely related phenomenon.

CONCLUSION

The importance of a spectrin meshwork in controlling shape and imparting strength and elasticity to the erythrocyte membrane has been recognized by many workers and is lucidly described by Steck [16]:

This matrix could offer the tough and inextensible skeletal support which the delicate and deformable fluid lipid bilayer (with its integrated proteins) might require to withstand the rigors of prolonged shear stress in the circulation. The "two-ply" structure created by the apposition of the fibrous meshwork to the supple lipid stratum might help account for the complex mechanical properties of the membranes observed in a variety of biophysical studies.

Rosenthal et al. [19] and Clarke and Griffith [54] have suggested that the

various Ca^{2+}-dependent, Mg^{2+}-stimulated ATPase activities that are extracted and co-purify with spectrin [55] could enzymatically modify the spectrin meshwork and thus alter the viscoelastic properties of the membrane. This would explain the observation that the inclusion of 1 mM ATP and Mg^{2+} during hypotonic lysis of human erythrocytes maintains the elastic deformability of the ghost membranes, while addition of as little as 0.1 mM Ca^{2+} renders the ghosts rigid [56]. However, the levels of these enzyme activities are very low, and Kirkpatrick et al. [55] have suggested instead that direct interaction of Ca^{2+} with spectrin could account for the observed changes.

Our own studies support this suggestion of Kirkpatrick et al. [55], and indicate that many of the phenomena observed in erythrocyte ghosts in response to their ionic environment, both morphological changes and alterations in the microscopic aggregation state of the intramembrane particles, can be explained by the physical behavior of solutions of spectrin and actin under similar conditions. In addition, the demonstration of a non-enzymatic, contractile process which leads to the production of protein-free lipid vesicles may be of significance in understanding phenomena such as pinocytosis, exocytosis and membrane fusion.

ACKNOWLEDGEMENTS

It is with great pleasure that we acknowledge our indebtedness to Eleanor Crump for her excellent assistance throughout these studies. We are especially grateful to our colleagues Leon Wofsy and Karen Thompson for the provision of antibody against phenyl lactoside and of the phenyl lactoside hapten, for their advice and assistance during the immunochemical labelling experiments, and for many stimulating discussions. We thank the blood bank of the Alameda-Contra Costa County Medical Association in Oakland, California, for gifts of outdated blood, David Cole for a sample of purified lysine-rich histone, and Michael Sheetz, Lewis Tilney and F. H. Kirkpatrick for sharing with us the results of their research prior to publication.

Arnljot Elgsaeter is grateful for a Haakon Styri Fellowship from the American-Scandinavian Foundation, a research fellowship from the Royal Norwegian Council of Scientific and Industrial Research, and a Fullbright Travelling Fellowship. David Shotton thanks the Medical Research Council of Great Britain for a Travelling Fellowship. This research was supported in part by grants and contracts to Daniel Branton from the U. S. National Institutes of Health, National Science Foundation, and Atomic Energy Commission.

REFERENCES

1 Marchesi, V. T., Steers, E., Tillack, T. W. and Marchesi, S. L. (1969) in Red Cell Membrane–Structure and Function (Jamieson, G. A. and Greenwalt, T. J., eds.), pp. 117–130, J. B. Lippincott
2 Marchesi, S. L., Steers, E., Marchesi, V. T. and Tillack, T. W. (1969) Biochemistry 9, 50–57
3 Tillack, T. W., Marchesi, S. L., Marchesi, V. T. and Steers, Jr., E. (1970) Biochim. Biophys. Acta 200, 125–131
4 Fairbanks, G., Steck, T. L. and Wallach, D. F. H. (1971) Biochemistry 10, 2606–2617
5 Clarke, M. (1971) Ph. D. Dissertation, University of California, Berkeley
6 Clarke, M. (1971) Biochem. Biophys. Res. Commun. 45, 1063–1070

7 Nicolson, G. L., Marchesi, V. T. and Singer, S. J. (1971) J. Cell Biol. 51, 265–272
8 Gwynne, J. T. and Tanford, C. (1970) J. Biol. Chem. 245, 3269–3271
9 Hulla, F. W. (1974) Biochim. Biophys. Acta 345, 430–438
10 Fuller, G. M., Boughter, J. M. and Morazzani, M. (1974) Biochemistry 13, 3036–3041
11 Steck, T. L. and Yu, J. (1973) J. Supramol. Struct. 1, 220–232
12 Allen, J. E. and Rasmussen, H. (1971) Science 174, 512–514
13 Evans, E. A. (1973) Biophys. J. 13, 926–940
14 Evans, E. A. (1973) Biophys. J. 13, 941–954
15 Kury, P. G., Ramwell, P. W. and McConnell, H. M. (1974) Biochem. Biophys. Res. Commun. 56, 478–483
16 Steck, T. L. (1974) J. Cell Biol. 62, 1–19
17 Tilney, L. G. and Detmers, P. (1975) J. Cell Biol. 66, 508–520
18 Hoogeveen, J. Th., Juniano, R., Coleman, J. and Rothstein, A. (1970) J. Membrane Biol. 3, 156–172
19 Rosenthal, A. S., Kregenow, F. M. and Moses, H. L. (1970) Biochim. Biophys. Acta 196, 254–262
20 Elgsaeter, A. and Branton, D. (1974) J. Cell Biol. 63, 1018–1030
21 Dodge, J. T., Mitchell, C. and Hanahan, D. J. (1963) Arch. Biochem. Biophys. 100, 119–130
22 Lowry, O. H., Rosebrough, N. J., Farr, A. L. and Randall, R. J. (1951) J. Biol. Chem. 193, 265–275
23 Fiske, C. H. and Subbarow, Y. (1925) J. Biol. Chem. 66, 375–400
24 Wofsy, L. and Burr, B. (1969) J. Immunol. 103, 380–382
25 Corneil, I. and Wofsy, L. (1967) Immunochemistry 4, 183–189
26 Wofsy, L., Baker, P. C., Thompson, K., Goodman, J., Kimura, J. and Henry, C. (1974) J. Exp. Med. 140, 523–537
27 Nicolson, G. L. and Singer, S. J. (1971) Proc. Natl. Acad. Sci. U.S. 68, 942–945
28 Nemanic, M. K., Carter, D. P., Pitelka, D. R. and Wofsy, L. (1975) J. Cell Biol. 64, 311–321
29 Truffa-Bachi, P. and Wofsy, L. (1970) Proc. Natl. Acad. Sci. U.S. 66, 685–692
30 Fisher, K. and Branton, D. (1974) Methods Enzymol. 32, 35–44
31 Moor, H. (1971) Phil. Trans. R. S. Lond. B 261, 121–131
32 Nicolson, G. L. and Painter, R. G. (1973) J. Cell Biol. 59, 395–406
33 Desnuelle, P. (1960) in The Enzymes (Boyer, P. D., Lardy, H. and Myrback, K., eds.), Vol. 4, p. 119, Academic Press, New York
34 Deamer, D. W., Leonard, R., Tardieu, A. and Branton, D. (1970) Biochim. Biophys. Acta 219, 47–60
35 Marchesi, V. T., Tillack, T. W., Jackson, R. L., Segrest, J. P. and Scott, R. E. (1972) Proc. Natl. Acad. Sci. U.S. 69, 1445–1449
36 James, R. and Branton, D. (1973) Biochim. Biophys. Acta 323, 378–390
37 Verkleij, A. J. (1975) Ph. D. Thesis, University of Utrecht
38 Kleemann, W. and McConnell, H. M. (1974) Biochim. Biophys. Acta 345, 220–230
39 Papahadjopoulos, D., Poste, G., Schaeffer, B. E. and Vail, W. J. (1974) Biochim. Biophys. Acta 352, 10–28
40 Jacobson, K. and Papahadjopoulos, D. (1975) Biochemistry 14, 152–161
41 Ji, T. H. and Nicolson, G. L. (1974) Proc. Natl. Acad. Sci. U.S. 71, 2212–2216
42 Hubbell, W. L. and McConnell, H. M. (1969) Proc. Natl. Acad. Sci. U.S. 64, 20–27
43 Wang, K. and Richards, F. M. (1974) J. Biol. Chem. 249, 8005–8018
44 Peters, R., Peters, J., Tews, K. H. and Bähr, W. (1974) Biochim. Biophys. Acta 367, 282–294
45 Singer, S. J. and Nicolson, G. L. (1972) Science 175, 720–731
46 Frye, L. D. and Edidin, M. (1970) J. Cell Sci. 7, 319–335
47 Cone, R. A. (1972) Nat. New Biol. 236, 39–43
48 Brown, P. K. (1972) Nat. New Biol. 236, 35–38
49 Poo, M. and Cone, R. A. (1974) Nature 247, 438–441
50 Bodemann, H. and Passow, H. (1972) J. Membrane Biol. 8, 1–26
51 Brown, J. N. and Harris, J. R. (1970) J. Ultrastruct. Res. 32, 405–416
52 Shin, B. C. and Carraway, K. L. (1973) J. Biol. Chem. 248, 1436–1444
53 Palek, J., Curby, W. A. and Lionetti, F. J. (1971) Am. J. Physiol. 220, 19–26
54 Clarke, M. and Griffith, J. (1972) Fed. Proc. 31, 412

55 Kirkpatrick, F. H., Woods, G. M., LaCelle, P. L. and Weed, R. I. (1975) J. Supramol. Struct., in the press
56 Weed, R. I., LaCelle, P. L. and Merrill, E. W. (1969) J. Clin. Invest. 48, 795–809
57 Eylar, E. H., Madoff, M. A., Brody, O. V. and Oncley, J. L. (1962) J. Biol. Chem. 237, 1992–2000
58 Sherbet, G. V., Lakshmi, M. S. and Rao, K. V. (1972) Exp. Cell Res. 70, 113–123
59 Southworth, D., Fisher, K. and Branton, D. (1975) in Techniques of Biochemical and Biophysical Morphology (Glick, D. and Rosenbaum, R., eds.), pp. 247–282, Wiley, New York